Int. J. Heat Mass Transfer. Vol. 17, pp. 517–525. Pergamon Press 1974. Printed in Great Britain

THE STABILITY OF THE LAMINAR FREE CONVECTION FLOW INDUCED BY A HEATED INCLINED PLATE

P. A. IYER and R. E. KELLY
Mechanics and Structures Department, School of Engineering and Applied Science,
University of California, Los Angeles, California 90024, U.S.A.

(*Received* 5 *May* 1972 *and in revised form* 7 *August* 1973)

Abstract—Visual observations by Lloyd and Sparrow [1] and Sparrow and Husar [2] have indicated that the instability of the boundary layer on a heated, inclined plate is predominated by two-dimensional waves for angles of inclination less than 14°, whereas both waves and longitudinal vortices are observed for angles of 14°–17°, and vortices predominate for larger angles. A linear stability analysis is carried out in this paper. It is found that each mode becomes unstable first at the same location along the plate at an angle of only 4°. However, correlation with the experimental observations is achieved by calculating the total amplification of each disturbance from the predicted point of onset of instability to the point of observed instability for various angles of inclination.

NOMENCLATURE

g, gravitational constant;
$\tilde{u}$, characteristic velocity in flow direction $\tilde{x}$;
v', vertical component of perturbation velocity;
$\tilde{x}$, dimensional distance along plate;
$\tilde{x}_0$, point of observed instability;
$\tilde{x}_1$, point of theoretical instability;
x, dimensionless distance along plate, $\tilde{x}/\delta$;
$\tilde{y}$, dimensional coordinate normal to plate, outwards;
$\tilde{z}$, dimensional coordinate spanwise on plate;
z, dimensionless coordinate spanwise on plate;
$Gr_{\tilde{x}}$, Grashof number based on $\tilde{x}$, $(\alpha_0 g \Delta T \tilde{x}/\nu_0^2)$;
Gr_δ, Grashof number based on boundary layer thickness, δ;
$\hat{G}r_\delta$, effective Grashof number, $Gr_\delta \tan\theta$;
$\hat{G}r_{\delta_c}$, critical effective Grashof number;
Pr, Prandtl number, ν_0/κ_0;
$Ra_{\tilde{x}}$, Rayleigh number based on $\tilde{x}$;
$Ra_{\tilde{x}_0}$, Rayleigh number at point of observed instability $\tilde{x}_0$;
Re_δ, Reynolds number based on boundary layer thickness, δ;
Re_{δ_c}, critical Reynolds number;
$\overline{U}$, basic flow velocity profile;
$\overline{T}$, basic temperature profile;
T_w, wall temperature;
T_0, ambient temperature;
T', perturbation temperature.

Greek symbols

δ, boundary layer thickness, $\sqrt{2}\tilde{x}/(Gr_{\tilde{x}}\cos\theta)^{1/4}$;
η, similarity variable, y/δ;
α_0, coefficient of volume expansion;
ν_0, kinematic viscosity;
κ_0, thermal diffusivity;
β, non-dimensional wavenumber in z direction;
α_i, spatial growth rate of travelling disturbances;
α_r, non-dimensional wavenumber in x direction;
α, complex wavenumber, $\alpha_r + i\alpha_i$;
$\tilde{\omega}$, dimensional frequency [Hz];
ω, non-dimensional frequency of travelling wave;
θ, inclination angle of plate from vertical;
γ, spatial growth rate of spanwise periodic disturbances;
$\tilde{\lambda}$, dimensional wavelength.

INTRODUCTION

BUOYANCY driven flows are of common occurrence in technological, atmospheric, and oceanic phenomena, the buoyancy stratification being achieved often by the temperature field. The stability of such flows therefore has considerable importance. This paper is concerned with the stability of flows over heated inclined surfaces located in an otherwise homogeneous medium.

Many previous investigations have been concerned with the stability of flows over heated vertical plates. As shown by Polymeropoulous and Gebhart [3], excellent correlations exist for this case between experimental results and theoretical predictions based on the parallel basic flow assumption. The instability for a vertical plate case occurs in the form of two-dimensional waves travelling in the streamwise direction. When the plate is inclined, however, another mode of instability is possible which manifests itself in the form of stationary longitudinal vortices, periodic in the spanwise direction. This mode of instability

arises due to the destabilizing influence of the buoyancy component normal to the inclined surface and is analogous to the Görtler vortices observed for flows over isothermal concave surfaces and caused by centrifugal forces (see Görtler [4], Hämmerlin [5], and Tani [6]). The analogy between centrifugal forces and buoyancy forces in causing instability was first discussed by Görtler [7]. Experiments by Sparrow and Husar [2] and by Lloyd and Sparrow [1] have indicated that an angle of tilt exists for which the longitudinal mode of instability becomes predominant. Working with a special dye-generation technique, for easy visual observations of the instability, they observed that when the angle of tilt was about 17° from the vertical, longitudinal vortices predominated the flow field, whereas for angles less than 14°, two-dimensional, travelling waves were predominant. No theoretical investigation has been done to date to correlate the results of linear stability theory with these experimental results, and this is the aim of the present paper. Only the above-mentioned form of disturbances were considered because these were the experimentally observed disturbances. We use a linear stability theory, assuming a parallel basic flow and a Boussinesq fluid with a Prandtl number of 6·7 (this Prandtl number being chosen in order to compare with the experimental data for water used by Lloyd and Sparrow [1]). The eigenvalue problem has been solved for both neutrally stable and spatially growing disturbances for various angles of inclination.

One way of defining the angle of modal transition is to find that angle at which both modes of instability begin to grow at the same point along the plate. For this criterion, only the neutral stability curve is required. However, such a result can only be compared meaningfully to data from an experiment in which truly small, controlled disturbances can be detected, such as in the work of Polymeropoulos and Gebhart [3]. This does not seem to be true in the experiments by Lloyd and Sparrow [1], in which visual observations of natural disturbances were made by use of a dye-technique. For instance, the Rayleigh number for the vertical case at which instability was first observed was given as $O(10^9)$ in their Table 1, whereas the critical value given by the theoretical analysis of Nachtsheim [8] is $O(10^5)$ for a Prandtl number of 6·7. This consideration becomes even more important for the present case, for which the spatial amplification of the travelling waves beyond the point of instability at the angle, as defined above, is significantly larger than that for longitudinal vortices. Hence, one can conceive of a situation in which the longitudinal vortices might begin to grow first, but for which the flow pattern further downstream would be dominated by the travelling waves. Growth rates were therefore calculated for various angles in order to estimate the total amplification of each disturbance over a given interval in $\tilde{x}$, and, as discussed in more detail below, to use this as a basis for comparison of theoretical and experimental results.

ANALYSIS

The system under consideration is shown in Fig. 1. A fluid of kinematic viscosity ν_0, thermal diffusivity κ_0, and coefficient of volume expansion α_0, occupies the region $\tilde{y} > 0$ bounded by a semi-infinite inclined wall at $\tilde{y} = 0$. The wall temperature T_W is greater than the temperature of the ambient fluid T_0, giving rise to a free-convection boundary layer flow. The angle of tilt measured from the vertical is θ, so that the streamwise component of gravity driving the flow is $g\cos\theta$. The similarity solutions for the basic velocity and temperature fields have been given by Ostrach [9] for a variety of Prandtl numbers for $\theta = 0°$. Numerical solutions for a Prandtl number 6·7 and $\theta = 0°$ have been given by Nachtsheim [8]. These solutions for the basic flow can be used for inclined plates as well, as shown by Kierkus [10], provided that the boundary layer scaling factor for the y-coordinate, δ, incorporates the effective gravitational constant and is defined as $\delta = \sqrt{2}\tilde{x}/(Gr_{\tilde{x}}\cos\theta)^{1/4}$, where $Gr_{\tilde{x}}$ is a Grashof number based on $\tilde{x}$, that $(Gr_{\tilde{x}}\cos\theta)^{1/4}$ is sufficiently large ($\gg 1$) so that higher order boundary layer corrections are negligible, and finally that $\tan\theta/(Gr_{\tilde{x}}\cos\theta)^{1/4}$ is sufficiently small so that the cross-stream buoyancy force can be ignored in the basic flow. If $(Gr_{\tilde{x}}\cos\theta)^{1/4} \gg 1$, the last requirement is certainly valid for $\tan\theta$ of order unity and so will be met for the angles ($\theta \approx 17°$) of primary interest here. We will assume that the boundary layer solutions of Nachtsheim [8] can be used with sufficient accuracy in the following analysis and will discuss the validity of this assumption later in the light of our stability results.

A linear stability analysis is used to study the stability of the boundary layer to two-dimensional travelling

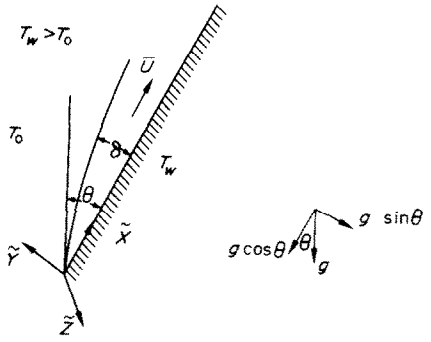

FIG. 1. The flow configuration.

waves periodic in the streamwise direction ($\tilde{x}$) and to stationary disturbances periodic in the spanwise direction ($\tilde{z}$). A Boussinesq fluid is considered, and the parallel flow assumption is made in the following analysis. The travelling waves will be investigated first.

The linear dimensionless stability equations for a vertical plate have been derived by Nachtsheim [8], and the derivation for an inclined plate is very similar. We use the following characteristic quantities in order to place the linear stability equations in non-dimensional form:

$$\text{length:} \quad \sqrt{2}\tilde{x}/(Gr_{\tilde{x}}\cos\theta)^{1/4} = \delta, \tag{1}$$

$$\text{velocity:} \quad 2\nu_0(Gr_{\tilde{x}}\cos\theta)^{1/2}/\tilde{x} = \tilde{u}, \tag{2}$$

$$\text{temperature:} \quad T_W - T_0 = \Delta T, \tag{3}$$

where

$$Gr_{\tilde{x}} = (\alpha_0 g \Delta T \tilde{x}^3)/\nu_0^2. \tag{4}$$

Tabulations of the mean flow $\overline{U}(\eta)$ and temperature distribution $\overline{T}(\eta)$ are given in Table 1 of Nachtsheim [8] in terms of the similarity variable $\eta = \tilde{y}/\delta$.

Assuming a vertical velocity and temperature disturbance of the form

$$v' = \hat{v}(\eta)\exp[i(\alpha x - \omega t)], \tag{5a}$$

$$T' = \hat{T}(\eta)\exp[i(\alpha x - \omega t)], \tag{5b}$$

we can derive through use of the momentum, continuity and energy equations, the governing stability equations as

$$(D^2 - \alpha^2 - i\alpha Re_\delta[\overline{U} - \omega/\alpha])(D^2 - \alpha^2)\hat{v} = i\alpha\tan\theta\hat{T} - i\alpha\overline{U}''Re_\delta\hat{v} - D\hat{T}, \tag{6}$$

and

$$(D^2 - \alpha^2 - i\alpha Re_\delta Pr[\overline{U} - \omega/\alpha])\hat{T} = -i\alpha\overline{T}'Re_\delta Pr\hat{v}, \tag{7}$$

where

$$Re_\delta = Gr_\delta = (\alpha_0 g \Delta T \delta^3 \cos\theta)/\nu_0^2$$

and

$$D = \mathrm{d}/\mathrm{d}\eta, \quad \overline{U} = \overline{U}(\eta), \quad \overline{T} = \overline{T}(\eta).$$

The boundary conditions are

$$\hat{v} = D\hat{v} = \hat{T} = 0 \quad \text{at} \quad n = 0, \tag{8a}$$

$$\hat{v} = D\hat{v} = \hat{T} = 0 \quad \text{as} \quad n \to \infty. \tag{8b}$$

Primes on basic flow quantities indicate derivatives with respect to η. The frequency of the disturbance is ω, and α is the complex wavenumber, the real part α_r representing the wavenumber and the imaginary part α_i representing the spatial growth rate ($\alpha_i > 0$ for decay and $\alpha_i < 0$ for growth).

The spanwise periodic stationary disturbances will now be considered. The derivation of the stability equations is similar to those for travelling waves. For a disturbance of the form

$$v' = \hat{v}(\eta)\exp[i\beta z + \gamma x], \tag{9}$$

the linear stability equations are

$$(D^2 - \beta^2 + \gamma^2 - \gamma Gr_\delta\overline{U})(D^2 - \beta^2 + \gamma^2)\hat{v} = \gamma D\hat{T} - \gamma Gr_\delta\overline{U}''\hat{v} - (\gamma^2 - \beta^2)\hat{T}\tan\theta \tag{10}$$

and

$$(D^2 - \beta^2 + \gamma^2 - Gr_\delta Pr\overline{U}\gamma)\hat{T} = \hat{v}\overline{T}'Gr_\delta Pr, \tag{11}$$

with the same boundary conditions as given in (8). β is real and represents a wavenumber in the spanwise direction, and $\gamma > 0$ represents the spatial growth rate of these disturbances. The disturbance as expressed above is non-oscillatory in time. Computer calculations were also done retaining frequency as a parameter, and it was found that the frequency is indeed zero within the numerical accuracy expected (i.e. of order 10^{-8}).

To distinguish between the two modes of instability, we associate the Reynolds number with the travelling wave mode and the Grashof number with the vortex mode, although both are equal.

METHOD OF SOLUTION

The stability equations for the travelling waves and stationary disturbances constitute in effect a sixth order differential equation with three boundary conditions at each end of the range of integration ($0 \leqslant \eta < \infty$). For travelling waves, the three independent solutions which satisfy the condition of decay, equation 8(b), as η tends to infinity behave like $\exp[i\lambda\eta]$ where λ has a positive imaginary part and satisfies the asymptotic form of the equations (6) and (7) for large η ($\overline{U} \to 0$, $\overline{U}' \to 0$, $\overline{T}' \to 0$), giving rise to the relation

$$(\lambda^2 + \alpha^2)(\lambda^2 + \alpha^2 - i\omega Re_\delta)(\lambda^2 + \alpha^2 - i\omega Re_\delta Pr) = 0. \tag{12}$$

If we associate λ_1, λ_2, λ_3 with the values of λ with positive imaginary parts obtained by solving the following equations,

$$\lambda_1^2 + \alpha^2 = 0, \tag{13a}$$

$$\lambda_2^2 + \alpha^2 - i\omega Re_\delta = 0, \tag{13b}$$

$$\lambda_3^2 + \alpha^2 - i\omega Re_\delta Pr = 0, \tag{13c}$$

three linearly independent solutions can be obtained by using the following starting conditions for large η

$$\hat{v}_1 = \mathrm{e}^{i\lambda_1\eta}, \quad \hat{v}_2 = \mathrm{e}^{i\lambda_2\eta},$$

$$\hat{v}_3 = \mathrm{e}^{i\lambda_3\eta}[(i\alpha\tan\theta - i\lambda_3)/(\lambda_3^2 + \alpha^2)(\lambda_3^2 + \alpha^2 - i\omega Re_\delta)], \tag{14a}$$

$$\hat{T}_1 = 0, \quad \hat{T}_2 = 0, \quad \hat{T}_3 = \mathrm{e}^{i\lambda_3\eta}, \tag{14b}$$

where the constant multiplying $\hat{v}_3$ is obtained from equation (6) for large η. For fixed values of wavenumber, angle of tilt, growth rates and an assumed Re_δ and ω, the integration is performed using Gill's modification of the fourth order Runge–Kutta method marching in from a large value of η to the wall ($\eta = 0$). A value of about 8·0 was found to be sufficiently large so as to represent effectively "infinity". (i.e. the results did not vary when larger values of η were used). A step size of 0·1 was used for the integration. Double precision arithmetic was used on an IBM 360/91 computer. The linear independence of the solutions was ensured by Gram–Schmidt orthonormalisation at every 10 steps of integration. The three solutions $(\hat{v}_1, \hat{T}_1)$, $(\hat{v}_2, \hat{T}_2)$, and $(\hat{v}_3, \hat{T}_3)$ were then combined at the wall using two arbitrary constants A and B as follows

$$\hat{v} = \hat{v}_1 + A\hat{v}_2 + B\hat{v}_3, \tag{15a}$$

$$D\hat{v} = D\hat{v}_1 + A(D\hat{v}_2) + B(D\hat{v}_3), \tag{15b}$$

$$\hat{T} = \hat{T}_1 + A\hat{T}_2 + B\hat{T}_3. \tag{15c}$$

The constants A and B were then evaluated to satisfy the wall conditions, $\hat{v}(0)$, $D\hat{v}(0)$. The third boundary condition at the wall, $\hat{T}(0) = 0$, was satisfied by converging on the right eigenvalues Re_δ and ω. A Newton–Raphson iteration technique was used to converge on the right eigenvalues. Excellent agreement was obtained for the vertical case ($\theta = 0$) with the results of Nactsheim [8] for transverse travelling waves.

For the case of longitudinal vortices, a similar procedure was followed, except that one must account for the repeated roots which arise from the equation analogous to equation (12). As a check of the method of solution, we verified Hammerlin's [5] result for the analogous case of centrifugal instability on a concave surface.

RESULTS AND DISCUSSION

Figure 2 shows the destabilizing effect on the tilt angle on the neutral curve for travelling waves. This effect is not just due to the $\cos^{1/4}\theta$ but represents the destabilizing influence of the additional energy provided to the disturbance through the buoyancy term in the momentum equation for the vertical disturbance component. The critical Reynolds number Re_{δ_c} is a function of θ, $Re_{\delta_c}(\theta)$, and decreases as θ increases, with a corresponding increase in critical wavenumber. For the flow on the underside of the plate, where stable stratification occurs, the results shown in Fig. 3 show that Re_{δ_c} tends to increase in a similar manner with θ, with a corresponding decrease in critical wavenumber.

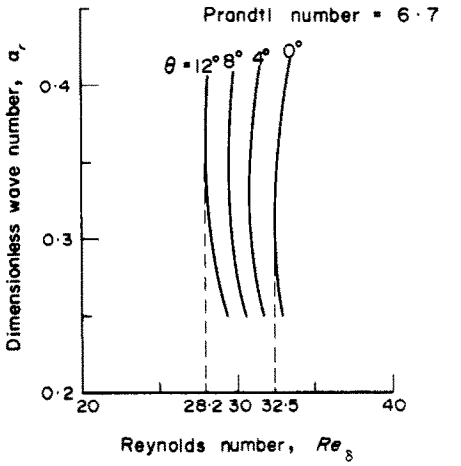

FIG. 2. Neutral curves for travelling disturbances as a function of inclination angle θ.

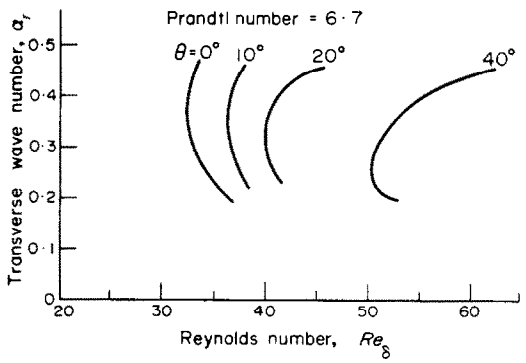

FIG. 3. Neutral curves for travelling disturbances as a function of inclination angle θ for the case of stable stratification.

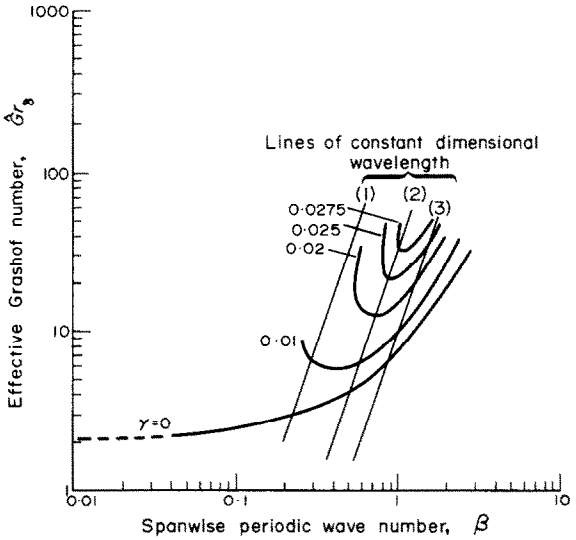

FIG. 4. Neutral curve and curves of constant spatial growth rate for longitudinal vortices for $\theta = 9{\cdot}2°$.

Figure 4 shows the neutral curve and curves of constant spatial growth rates for spanwise periodic disturbances, as functions of wavenumber β and the effective Grashof number for thermal instability $\hat{G}r_\delta = Gr_\delta \tan\theta$, for a tilt angle of 9·2° from the vertical. Only the neutral curve is independent of θ. The curve asymptotes towards a spanwise wavenumber of zero, a result analogous to that of Hämmerlin [5] for the case of Görtler vortices, and the critical effective Grashof number $\hat{G}r_{\delta_c}$ equals 2·15. Since Gr_{δ_c} is independent of θ, and Gr_δ is constant as θ increases only if $\tilde{x}$ decreases, it can be seen that as the plate is inclined away from the vertical, the point along the plate at which the longitudinal disturbances first become unstable moves towards the leading edge and at some angle, θ_N, becomes equal to the point at which the travelling waves first become unstable. For $\theta > \theta_N$, the longitudinal disturbances become unstable first. This angle can be obtained from the equation

$$\tan\theta = 2{\cdot}15/Re_{\delta_c}(\theta), \tag{16}$$

remembering that $Gr_\delta = Re_\delta$, by use of the results given in Fig. 2 for $Re_{\delta_c}(\theta)$.

When this is done, the angle θ_N for transition from the travelling mode to the longitudinal mode is found to be only 4°, a value rather low when compared to the experimentally observed value of approximately 17°. However, the critical Grashof number occurs for low wavenumber longitudinal disturbances which then grow very slowly along the plate. In contrast, the travelling waves can grow more rapidly and thereby dominate the flow within a short distance of the point of instability, thus becoming visible first. A more realistic test of the theory therefore arises from calculating the total amplification of each mode from the point of onset of instability to the point of observed instability and to see which mode predominates. If the amplitudes are comparable for an angle of approximately 17°, the use of linear stability theory is meaningful and consistent with the experimental results. The amplitude ratios for the disturbances as a function of x are given by

$$\left|\frac{A_2}{A_1}\right| = \exp\left[\frac{1}{3}\int_{Re_{\delta_1}}^{Re_{\delta_2}} (-\alpha_i)\,dRe_\delta\right] \tag{17}$$

for travelling disturbances and

$$\left|\frac{A_2}{A_1}\right| = \exp\left[\frac{1}{3\tan\theta}\int_{\hat{G}r_{\delta_1}}^{\hat{G}r_{\delta_2}} \gamma\,d\hat{G}r_\delta\right] \tag{18}$$

for stationary longitudinal vortices.

Figures 5 and 6 show the neutral curves and curves of constant spatial growth rates for $\theta = 16°$ for travelling disturbances and stationary vortices, respectively. Similar curves were obtained for $\theta = 9{\cdot}2°$ (Figs. 7 and 4). Superimposed on these are lines of constant dimensional frequency in Fig. 5 and lines of constant dimensional wavelength in Fig. 6, which indicate the path followed by such disturbances as they progress into the boundary layer. The amplitude ratios as a function of $\tilde{x}$ were then calculated by integration along these lines using equations (17) and (18). Such calculations are meaningful in view of the observations of Lloyd and Sparrow, who found more or less regularly spaced lines parallel to the streamwise direction, indicating that the dimensional wavelength remains constant with $\tilde{x}$. Similar observations were made by Tani [6] for the case of Görtler vortices. The results

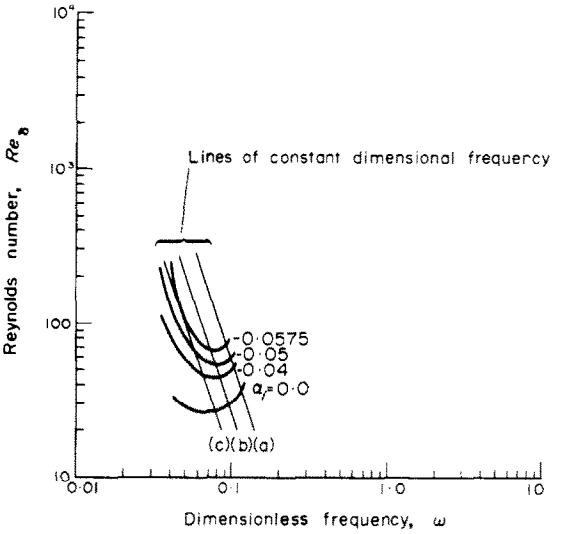

FIG. 5. Neutral curve and curves of constant spatial growth rate for travelling waves for $\theta = 16°$.

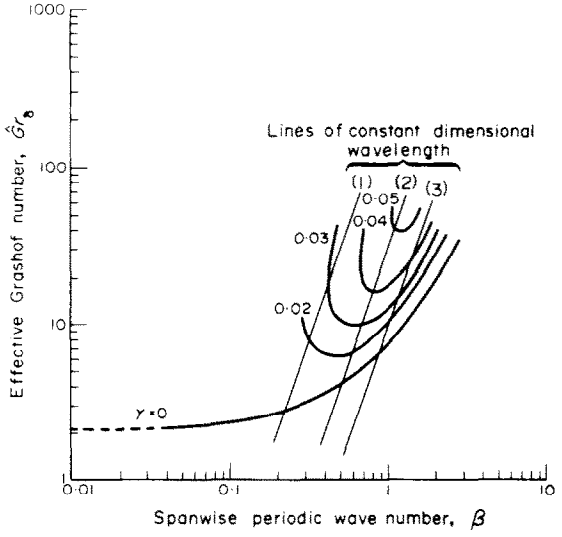

FIG. 6. Neutral curve and curves of constant spatial growth rate for longitudinal disturbances for $\theta = 16°$.

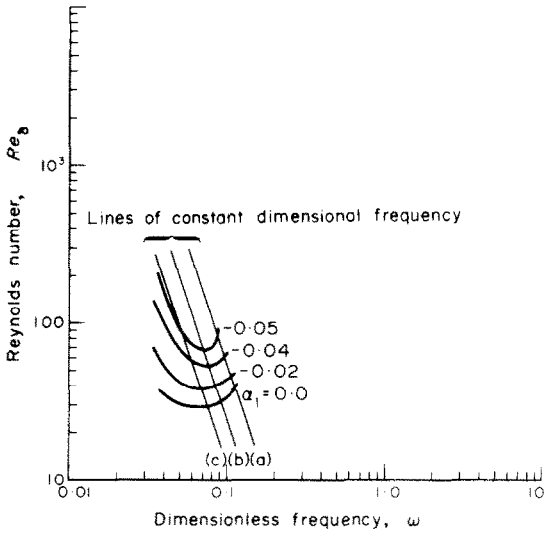

FIG. 7. Neutral curve and curves of constant spatial growth rate for travelling waves for $\theta = 9{\cdot}2^\circ$.

of the integration are plotted in Fig. 8 for $\theta = 9{\cdot}2^\circ$ and in Fig. 9 for $\theta = 16^\circ$ as a function of Rayleigh Number $Ra_{\tilde{x}}$ based on $\tilde{x}$, for the disturbance which achieves the largest amplitude ratio at the location along the plate at which disturbances were observed. The distance from the leading edge at which the disturbances were observed, $\tilde{x}_0$, was obtained from the mean Rayleigh numbers reported by Lloyd and Sparrow [1], assuming a Prandtl number of 6·7. Their Fig. 1 suggests that the curve of Rayleigh number for observed instability versus angle of inclination is reasonably insensitive to Prandtl number variations. It is clear from Fig. 8 that for $\theta = 9{\cdot}2^\circ$ the travelling waves achieve an amplitude ratio $|A_2/A_1| = 51{\cdot}0$ which is about 9·0 times larger than the ratio $|A_2/A_1| = 5{\cdot}7$ for longitudinal disturbances, both evaluated at the observed point of instability $Ra_{\tilde{x}_0} = 4{\cdot}8 \times 10^8$. The travelling waves consequently still predominate the observed instability. For $\theta = 16^\circ$ (Fig. 9), the travelling waves achieve an amplitude ratio $|A_2/A_1| = 43{\cdot}5$ compared to 28·0 for longitudinal disturbances at the observed point of instability $Ra_{\tilde{x}_0} = 3{\cdot}3 \times 10^8$. Thus the ratios differ by only a factor of 1·5. The values can be considered to be close, especially when we consider the 25 per cent standard deviations from the mean Rayleigh numbers reported by Lloyd and Sparrow. For $\theta = 35^\circ$, the results shown in Fig. 10 indicate that the longitudinal disturbances achieve an amplitude ratio about 6 times the amplitude ratio achieved by the travelling waves at the observed point of instability. The longitudinal vortices will consequently predominate the observed instability. The results for $\theta = 35^\circ$, however, should be interpreted with caution, because, as discussed later, the parallel flow assumption is in question for this high inclination angle.

The theoretical results, based on the parallel flow assumption and linear stability theory therefore appear to yield results which are quite consistent with the experimental results, at least as far as predicting the predominant mode at a given angle of inclination is concerned. However, they also indicate that a definition

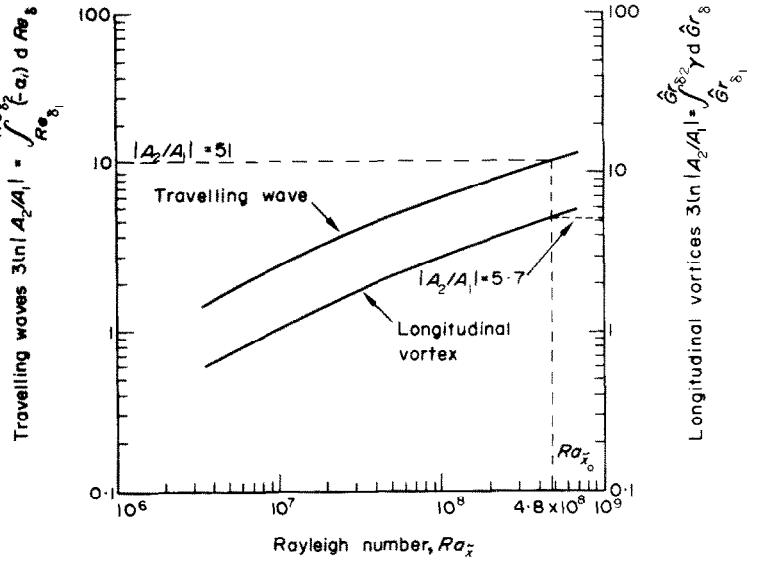

FIG. 8. Amplitude ratios as a function of $Ra_{\tilde{x}}$ for $\theta = 9{\cdot}2$ for travelling waves and longitudinal vortices.

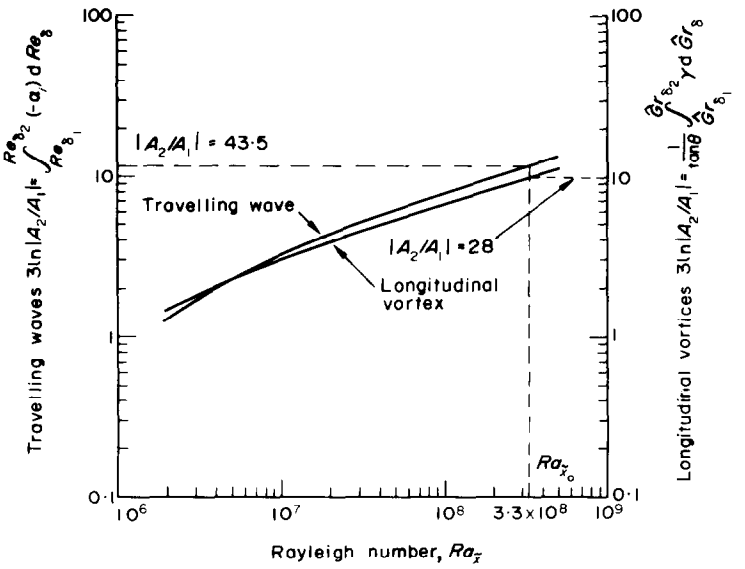

FIG. 9. Amplitude ratios as a function of $Ra_{\bar{x}}$ for $\theta = 16$ for travelling waves and longitudinal vortices.

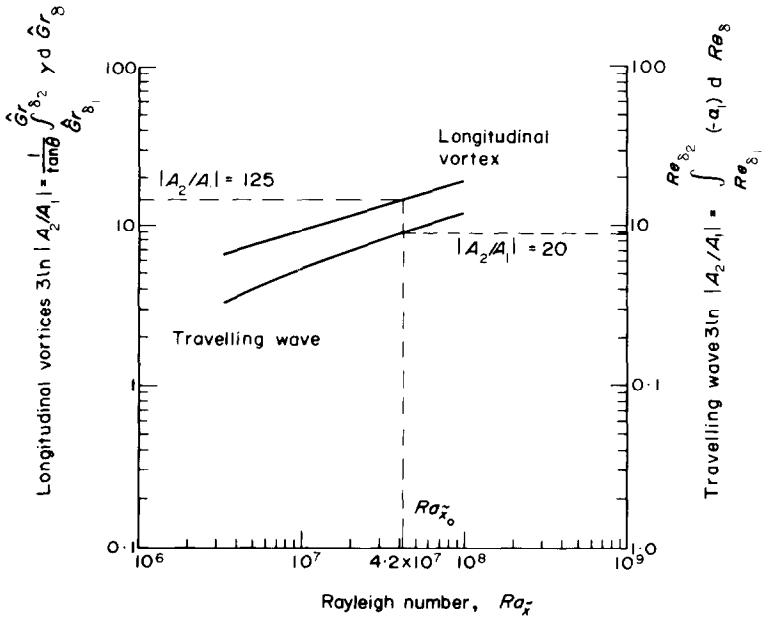

FIG. 10. Amplitude ratio as a function of $Ra_{\bar{x}}$ for $\theta = 35$ for longitudinal vortices.

of an angle of transition between modes is rather nebulous from an experimental viewpoint, depending strongly upon the experimentalist's ability to detect small disturbances and disturbance amplitudes which are of concern.

The dimensional frequencies and wavelengths reported in the figures have been calculated for $\Delta T = 28°C$ and for physical properties of the fluid corresponding to a Prandtl number of 6·7. It can be shown that the dimensional frequency and wavelength are given by the relations

$$\tilde{\omega} = \frac{\omega}{2\pi}\left[\frac{\alpha_0 g \Delta T \cos\theta}{\nu_0^2}\right]^{2/3} (Gr_\delta)^{1/3}\nu_0 \qquad (19)$$

and

$$\tilde{\lambda} = \frac{2\pi}{\beta}\left[\frac{\alpha_0 g \Delta T \sin\theta}{\nu_0^2}\right]^{-1/3} (Gr_\delta \tan\theta)^{1/3}. \qquad (20)$$

The data on the observed wavelength of longitudinal vortices is very meager. Sparrow and Husar reported that the number of dye lines observed (distance between two dye lines being equivalent to a wavelength) for a fixed angle $\theta = 35°$ increased from 30 to 42 as ΔT was increased from 9° to 28°C. On a spanwise width of 20 cm, this represents a wavelength of 0·475 cm for $\theta = 35°$ and $\Delta T = 28°C$. The distance from the leading edge at which the instability was observed, deduced from the mean Rayleigh numbers reported by Lloyd and Sparrow, is equal to 4·6 cm for $\Delta T = 28°C$, and corresponds to a Rayleigh number $Ra_{\tilde{x}_0} = 4{\cdot}2 \times 10^7$. Figure 10 shows the amplitude ratios for the most amplified longitudinal disturbances for $\theta = 35°$ as function of Rayleigh number $Ra_{\tilde{x}}$: The wavelengths of these disturbances vary between 0·48 cm and 0·68 cm, the curves corresponding to these wavelengths being found to be very close to each other. This represents reasonable correlation with experiments, considering the assumptions of the theory.

The parallel flow assumption made in the above analysis will be reviewed in light of the stability results. The values of the expansion parameter $(Gr_{\tilde{x}} \cos\theta)^{-1/4}$ used in the perturbation analysis of Kierkus [10] is given in Table 1 for various angles of inclination for both modes of instability. It can be seen that for travelling waves the value of $(Gr_{\tilde{x}} \cos\theta)^{-1/4}$ is of the order of 0·1 or less for the whole range from $\tilde{x}_1$ to $\tilde{x}_0$. Since the non-parallel flow terms are of this order, it seems reasonable to neglect these terms in preference to the convective parallel flow terms which are of order unity. For longitudinal vortices, however, the non-parallel flow terms become important especially near $\tilde{x}_1$ and, for $\theta = 35°$, the assumption is particularly bad. Also near $\tilde{x}_1$ and hence near the neutral curve the growth rates are of order $(Gr_{\tilde{x}} \cos\theta)^{-1/4}$ or less, and the stability analysis should be modified to include the non-parallel flow terms in order to define the neutral stability point. The value of Gr_{δ_c} might then occur for a non-zero wavenumber. The reasonably successful correlation of theoretical and observed wavelengths at $\theta = 35°$, reported earlier, was presumably obtained by computing over an interval for which the parallel flow assumption becomes increasingly more valid.

Table 1. Expansion parameter $(Gr_{\tilde{x}} \cos\theta)^{-1/4}$ as a function of θ and $\tilde{x}$, for $\Delta T = 28°C$
$\tilde{x}_1$ = point of theoretical instability
$\tilde{x}_0$ = point of observed instability

	Travelling waves		Longitudinal vortices	
	$\theta = 0°$	$\theta = 16°$	$\theta = 16°$	$\theta = 35°$
$\tilde{x}_1$ cm	0·65	0·5	0·25	0·074
$(Gr_{\tilde{x}_1} \cos\theta)^{-1/4}$	0·087	0·105	0·2	0·47
$\tilde{x}_0$ cm	10·34	9·15	9·15	4·6
$(Gr_{\tilde{x}_0} \cos\theta)^{-1/4}$	0·0109	0·0122	0·0122	0·021

Acknowledgement—This work has been supported by the National Science Foundation through Grant GA-31247 and by the U.S. Army Research Office—Durham.

REFERENCES

1. J. R. Lloyd and E. M. Sparrow, On the instability of natural convection flow on inclined plates, *J. Fluid Mech.* **42**, 465–470 (1970).
2. E. M. Sparrow and R. B. Husar, Longitudinal vortices in natural convection flow on inclined plates, *J. Fluid Mech.* **37**, 251–255 (1969).
3. C. E. Polymeropoulos and B. Gebhart, Incipient instability in free convection laminar boundary layers, *J. Fluid Mech.* **30**, 225–239 (1967).
4. H. Görtler, On the three dimensional instability of laminar boundary layers on concave walls, NACA TM 1375 (1954).
5. G. Hämmerlin, Uber das Eigenwertproblem der dreidimensionalen instabilitat laminarer Grenzschichten an Konkaven Wanden, *J. Rat. Mech. Anal.* **4**, 279–321 (1955).
6. I. Tani, Production of longitudinal vortices in the boundary layers along a concave wall, *J. Geophys. Res.* **67**, 3075–3080 (1962).
7. H. Görtler, Uber eine Analogie Zwischen den instabilitaten laminarer Grenzschichtstromungen an Konkaven Wanden und an enwarmten Wanden, *Ing. Arch.* **38**, 71–78 (1959).
8. P. R. Nachtsheim, Stability of free convection boundary layer flows, NASA TN-D-2089 (1963).
9. S. Ostrach, An analysis of laminar free convection flow and heat transfer about a flat plate parallel to the direction of the generating body force, NACA Rep. 1111 (1953).
10. W. T. Kierkus, An analysis of laminar free convection flow and heat transfer about an inclined isothermal plate, *Int. J. Heat Mass Transfer* **11**, 241–253 (1968).

STABILITE DE LA CONVECTION LAMINAIRE NATURELLE INDUITE PAR UNE PLAQUE CHAUFFEE ET INCLINEE

Résumé—Des visualisations réalisées par Lloyd et Sparrow [1] et Sparrow et Husar [2] ont montré que l'instabilité de la couche limite sur une plaque chauffée et inclinée est marquée par des ondes bidimensionnelles pour des angles d'inclinaison inférieurs à 14°, par des ondes et des tourbillons longitudinaux entre 14 et 17°, tandis que les tourbillons prédominent pour les angles plus grands. On développe dans cet article une analyse de stabilité linéaire. On trouve que chaque mode devient instable au même endroit sur la plaque pour un angle de 4° seulement. Néanmoins on obtient un accord avec les observations expérimentales en calculant l'amplification totale de chaque perturbation depuis le point calculé du déclanchement de l'instabilité jusqu'au point d'instabilité observé, pour différents angles d'inclinaison.

DIE STABILITÄT EINER LAMINAREN FREIEN KONVEKTIONSSTRÖMUNG AN EINER GEHEIZTEN, GENEIGTEN PLATTE

Zusammenfassung—Optische Beobachtungen durch Lloyd und Sparrow [1] und Sparrow und Husar [2] haben gezeigt, daß die Instabilität der Grenzschicht an einer geheizten, geneigten Platte überwiegend durch zweidimensionale Wellen für Neigungswinkel kleiner als, 14° auftritt. Daher werden sowohl Wellen als auch Längswirbel für Winkel zwischen 14 und 17° beobachtet, während für größere Winkel Wirbel vorherrschen. Eine lineare Stabilitätsuntersuchung ist angegeben, Es zeigt sich, daß jede Konfiguration an der gleichen Stelle der Platte bei einem Winkel von nur 4° instabil wird. Eine Korrelation der Versuchsergebnisse wird erreicht durch Berechnung der Gesamtausbreitung jeder Strömung von der vorhergesagten zur beobachteten Störstelle bei verschiedenen Neigungswinkeln.

УСТОЙЧИВОСТЬ ЛАМИНАРНОГО ТЕЧЕНИЯ ПРИ СВОБОДНОЙ КОНВЕКЦИИ НА НАГРЕТОЙ НАКЛОННОЙ ПЛАСТИНЕ

Аннотация — Визуальные наблюдения, проведенные Ллойдом и Спэрроу [1], Спэрроу и Хузаром [2], показали, что неустойчивость пограничного слоя на нагретой наклонной пластине обуславливается двумерными волнами при углах наклона меньше 14°. Для углов 14–17° наблюдаются как волны, так и продольные вихри, а при больших углах преобладают вихри. В данной работе выполнен линейный анализ устойчивости. Найдено, что каждая мода становится первоначально неустойчивой в одной и той же точке на пластине только при угле 4°. Соответствие с экспериментальными наблюдениями достигнуто путём расчёта общего усиления каждого возмущения от расчётной точки возникновения неустойчивости до точки наблюдаемой неустойчивости при различных углах наклона.